REPORT DOCUMENTATION PAGE

Form Approved
OMB No. 0704-0188

1. REPORT DATE *(DD-MM-YYYY)*	**2. Report Type:**	**3. DATES COVERED** *(From - To)*
01-02-2001	Journal Article	N/A

4. TITLE AND SUBTITLE
A Low-Sidelobe Partially Overlapped Constrained Feed Network for Time-Delayed Subarrays

5a. CONTRACT NUMBER
In-House

5b. GRANT NUMBER
N/A

5c. PROGRAM ELEMENT NUMBER
61102F

6. AUTHOR(S)

Robert J. Mailloux

5d. PROJECT NUMBER
2304

5e. TASK NUMBER
HA

5f. WORK UNIT NUMBER
01

7. PERFORMING ORGANIZATION NAME(S) AND ADDRESS(ES)
N/A

8. PERFORMING ORGANIZATION REPORT

N/A

9. SPONSORING / MONITORING AGENCY NAME(S) AND ADDRESS(ES)
Electromagnetics Technology Division
Sensors Directorate Source Code 437890
Air Force Research Laboratory
80 Scott Drive
Hanscom AFB MA 01731-2909

10. SPONSOR/MONITOR'S ACRONYM(S)
AFRL-SN-HS

11. SPONSOR/MONITOR'S REPORT NUMBER(S)

AFRL-SN-HS-TP-2001-1485

12. DISTRIBUTION / AVAILABILITY STATEMENT
Statement A: Approved for Public Release; distribution unlimited; ESC 01-1485

13. SUPPLEMENTARY NOTES
AFSOR LRIR 925NOZCOR; IEEE Transactions on Antennas and Propagation, Vol. 49, No. 2, February 2001

14. ABSTRACT

Completely overlapped space-fed subarrays have been shown to provide sufficient pattern control to enable (modestly) wide-band arrays using time delays at the input to each subarray and phase shifters at the array face. These configurations are bulky, but have been proposed for space-based use as well as for certain ground-based applications that do not have severe volume constraints. Other applications for space-based and airborne radar require much more compact, constrained array feed networks, but until now there have been few appropriate constrained networks for inserting time delay at the subarray ports without causing high sidelobes. This paper describes one such network that, at the outset, provided far lower sidelobes than the usual contiguous subarrays, but retained closely spaced high lobes near the main beam. This paper presents a synthesis procedure that alters the subarray pattern and reduces nearly all array sidelobes to levels determined by tolerance errors. Several examples are presented that synthesize sidelobes at -40 dB. The resulting network operates over 70% to 80% of the maximum theoretical bandwidth.

15. SUBJECT TERMS
antennas, phased arrays, pattern synthesis, constrained-feed networks

16. SECURITY CLASSIFICATION OF:			**17.LIMITATION OF ABSTRACT**	**18.NUMBER OF PAGES**	**19a. NAME OF RESPONSIBLE PERSON**
Unclassified					Dr. Scott G. Santarelli
a. REPORT	**b. ABSTRACT**	**c. THIS PAGE**	UU	**13**	**19b. TELEPHONE NUMBER** *(include area code)*
Unclassified	Unclassified	Unclassified			N/A

Standard Form 298 (Rev. 8-98)
Prescribed by ANSI Std. Z39.18

A Low-Sidelobe Partially Overlapped Constrained Feed Network for Time-Delayed Subarrays

Robert J. Mailloux, *Fellow, IEEE*

***Abstract*—Completely overlapped space-fed subarrays have been shown to provide sufficient pattern control to enable (modestly) wide-band arrays using time delays at the input to each subarray and phase shifters at the array face. These configurations are bulky, but have been proposed for space-based use as well as for certain ground-based applications that do not have severe volume constraints. Other applications for space-based and airborne radar require much more compact, constrained array feed networks, but until now there have been few appropriate constrained networks for inserting time delay at the subarray ports without causing high sidelobes. This paper describes one such network that, at the outset, provided far lower sidelobes than the usual contiguous subarrays, but retained closely spaced high lobes near the main beam. This paper presents a synthesis procedure that alters the subarray patterns and reduces nearly all array sidelobes to levels determined by tolerance errors. Several examples are presented that synthesize sidelobes at −40 dB. The resulting network operates over 70% to 80% of the maximum theoretical bandwidth.**

***Index Terms*—Antenna feeds, beamsteering, phased arrays.**

I. Introduction

ELEMENTS of large arrays are often grouped into subarrays for the purpose of decreasing the array feed complexity or reducing the number of controls. There is an increasing need for efficient, high-quality subarraying techniques in systems that scan over a limited field of view (LFOV), and also in the wide-band systems that are the subject of this paper. Wide-band scanning systems use phase shifters at each element and analog time-delay units or digital receivers at the subarray level, so there is a cost savings resulting from the use of fewer, larger subarrays and an accompanying reduction in the number of time-delay devices. In this case, the maximum subarray size D_0 for an array with very narrow beamwidth is approximately given by $D_0/\lambda_0 = f_0/(\Delta f \sin(\theta_{\max}))$, where $(\Delta f/f_0)$ is the fractional bandwidth. In the best practical cases, a subarray size of 70%–80% of the maximum spacing is usually an upper limit, and this is only approached using space-fed overlapped subarray techniques that achieve grating lobe suppression by forming flat-topped subarray patterns.

Space-fed subarray systems use a Butler matrix or small focusing lens to excite an array of feed elements at the focus of a larger reflector or lens aperture. If the array is large enough to require more subarrays, one must build a larger aperture, excited by a larger feed array with more multiple beam ports. This requires more depth and volume, and may not be an acceptable solution for systems with volume constraints, including vehicle mounted ground arrays, airborne scanning arrays and some space applications. There is a fundamental need for subarray techniques that allow low sidelobe patterns to be formed and scanned and that have compact volume.

The most compact subarraying arrangement for large subarrays is the use of contiguous, uniformly illuminated, in-phase subarrays fed by constrained corporate power dividers. This kind of subarray is replicated across the large array, thus simplifying fabrication. The array is steered using phase shift at all elements and time-delay behind each subarray. The difficulty with arrays so constructed is that, at frequencies other than center frequency, they have many large grating lobes, often called "quantization lobes," and this limits their use to systems that have essentially no peak sidelobe constraints.

A number of useful compact (constrained) networks have been developed for forming overlapped subarrays. These networks are described in texts and survey references [1]–[3] and comprise a significant body of work. They are primarily applicable to relatively smaller subarrays (of 6 or 8 elements) because the network complexity increases with subarray size. In addition, they usually have sidelobes with lower limit on the order of −20 dB.

We have previously reported two constrained network schemes to form the larger subarrays required for time-delayed systems. The basic subarrays are formed with fully constrained networks consisting of Butler or Blass matrices, Rotman lenses or other beamformers, and simple power-combining networks. These constrained networks, called sections, may include several subarrays, but have far fewer outputs than the final array. Their size may be a third or a quarter or a smaller fraction of the size of the final array. The first technique introduced [4] was to simply abut these sections, placing them contiguously across the array. This contiguous array of overlapped subarrays does provide a relatively simple solution that is physically compact, but has a wide region of sidelobes at approximately the −20-dB level. It will not be discussed further here.

The second technique [4], [5] is a new way of partially overlapping these overlapped subarray sections. This paper presents the theoretical basis for this new technique, but more importantly develops methods of sidelobe control that make this an approach that can produce patterns with sidelobes at the −40-dB level, and potentially lower.

Fig. 1 explains the motivation for introducing this new technique by comparing it with an array of contiguous subarrays.

Manuscript received February 8, 2000; revised July 27, 2000. This work was supported by the Air Force Office of Scientific Research, Mathematics and Space Sciences Directorate under Dr. A. Nachman.

The author is with the Sensors Directorate, Air Force Research Laboratory, Hanscom AFB, MA 01731-2909 USA.

Publisher Item Identifier S 0018-926X(01)01267-4.

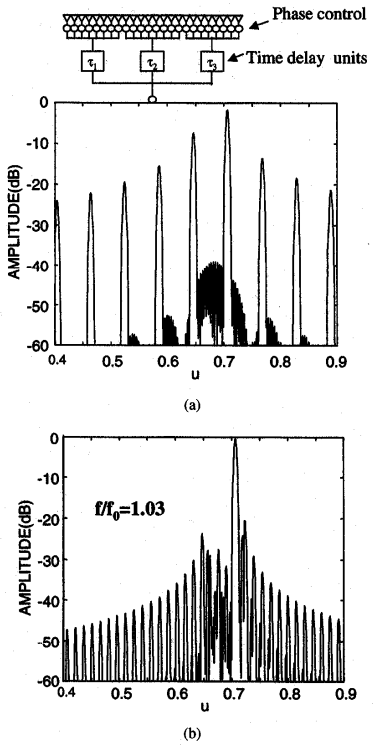

Fig. 1. Comparison of radiation patterns for arrays of 16 subarrays with 32 elements each. (a) Pattern of contiguous subarrays. (b) Pattern of partially overlapped sections of overlapped subarrays.

Fig. 1(a) shows the pattern an array of contiguous uniformly illuminated subarrays, like those shown schematically in the sketch at the top of the figure. An amplitude taper is used at the subarray input terminals, so that the basic array factor is a -40-dB Taylor pattern. In this example, the elements are spaced one half wavelength apart. The array is scanned to 45° and consists of sixteen subarrays, each 16 wavelengths in extent, and with 32 elements per subarray. There are phase shifters at each element and one time delay per subarray. The frequency is 1.03 times the center frequency, signifying the upper edge of a 6% bandwidth system. The center frequency case is not shown since it has only small grating lobes due to the quantized amplitude taper and is otherwise the same as the 40-dB Taylor pattern. Notice that there is a significant spectrum of grating lobes at levels that would be intolerable for some systems.

For comparison, Fig. 1(b) shows initial results of the new technique presented in [4] and [5], and demonstrates significant suppression of the grating lobes that were evident in the contiguous subarray case. Although the quantization lobes are significantly reduced, there are more of them, and the ones near the main beam are about -20 dB. This paper shows that these near sidelobes result from the subarrays being different, but correlated within groups, thus forming a higher order (spatially longer) periodicity across the array. This phenomenon is not present in any earlier subarraying technologies, but results from the partially overlapped distribution introduced by this new technique. The paper presents a synthesis technique that makes all the subarrays nearly identical and so removes this higher order periodicity.

II. Partially Overlapped Sections of Overlapped Subarrays

Fig. 2 depicts the technique for using constrained feed overlapped subarray networks as "sections" of a larger array. The makeup of these sections is described briefly in the next paragraphs. The new concept partially overlaps the output of these sections by first producing more subarrays than needed, discarding the ones nearest the edge of each section, and combining the remaining subarrays to produce well-controlled, low sidelobe patterns. Although the sketch shows only three sections with four subarrays each, the array may have numerous sections and each section may have more subarrays. In fact, this is seen as one of the advantages of the scheme, in that additional identical sections may be added to form a larger array with no change in the design of the basic section. In addition, it is shown in this paper that the subarrays can be further modified for sidelobe improvement, even within the passband of the subarray pattern.

The basic component of this technology is called a "section" and, as shown in Fig. 3, is an overlapped subarray network. This means that two focusing systems (one much larger than the other) are used back to back. In this case, we are only concerned with systems that can replace a corporate feed in an array architecture, so it will be assumed that the larger focusing system is a multiple beam lens, like a Rotman or other lens implemented in parallel plate or microstrip or stripline (or optical fiber), or a constrained multiple beam network like a true time-delay Blass matrix. This larger beamformer has N output terminals and M input terminals (with $M \ll N$). In normal use, the N output terminals would be connected to antenna elements, and a signal applied to one of the input terminals would result in a progressive phase shift across the elements. Other inputs have other rates of phase progression, corresponding to radiating beams in different directions. Exciting this multiple beam lens with a second, smaller focussing system, which could be a Butler matrix, a lens, or a digital Fourier transform, causes each input to the smaller network to produce a sinc-like distribution (or subarray) across all N output terminals of the larger beamformer. Adjacent subarrays are spaced a distance D_0 between centers at center frequency. Each of these overlapped distributions radiates with a pulse-shaped radiation pattern of width λ/D_0 rad at center frequency that performs the required grating lobe suppression.

Fig. 2 illustrates several aspects of the new subarraying feed concept. Three identical subarraying sections are depicted, and the output terminals of the sections are combined in the manner shown. Each section is a dual transform network that forms the overlapped distributions shown aside of that section. To simplify this illustrative example, each section is depicted as having

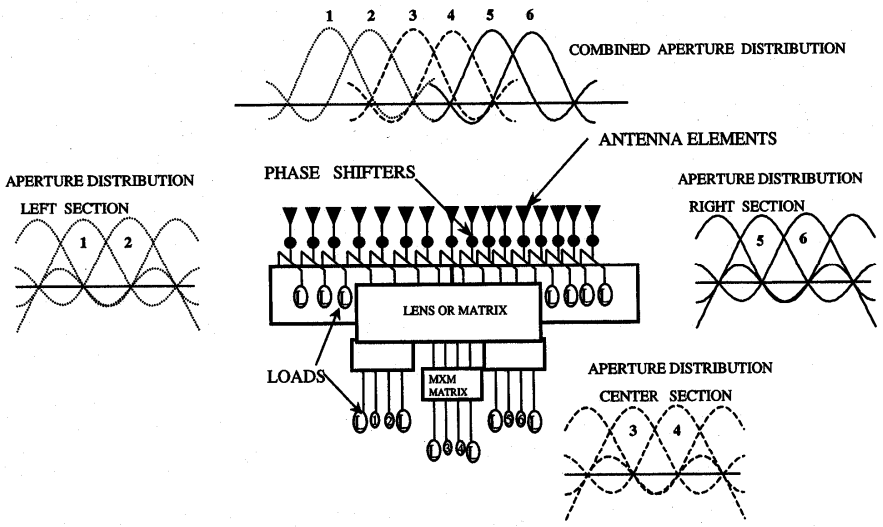

Fig. 2. Partially overlapped sections of overlapped subarrays.

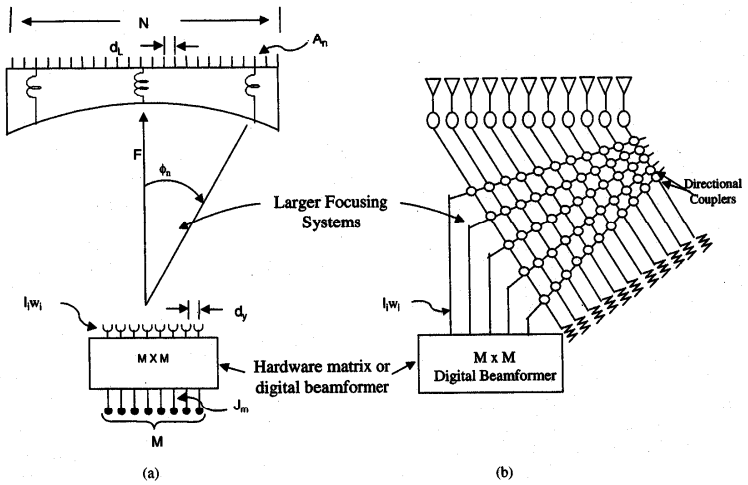

Fig. 3. Alternative transform networks for feeding a section of the array. (a) Lens and transform feed. (b) Constrained Blass time-delayed multiple-beam network and digital beamformer.

only four subarray illuminations ($M = 4$). Notice that the edge subarray illuminations are truncated, while the two center subarray illuminations of each section have the central region and at least one sidelobe of the amplitude distribution. Shown in a later figure, the associated subarray patterns of the central subarrays are a better approximation to the pulse-shaped ideal pattern. Implementation of this technique proceeds as indicated of the figure, where dotted, dashed and solid lines show the numbered subarrays formed by the left, center and right sections. The combined illumination therefore uses only the best of the subarrays, to produce the best grating lobe suppression. The edge subarrays that are omitted are replaced by central subarrays of other sections as shown in Fig. 2. The addition network introduces approximately a 3-dB loss in the hybrid power divider/combiners.

For this reason, the concept is primarily useful after amplification on receive and before amplification on transmit. This is not a significant limitation if the network is used to control a system with only one plane of scan, or an array of columns. Most such corporate feed approaches need amplification at columns to compensate loss in feed and phase shifter and/or time-delay devices, and so the 3-dB loss may be of little consequence.

This description has presented the basic technique and suggests its potential for good pattern control, however, as presented in [4] and [5] the original configuration does not meet the standard of low to very low sidelobes. This paper presents a technique to synthesize excellent low sidelobe patterns using this new subarray network.

A. Analysis of One Section

Each "section" of this array is a conventional overlapped subarray beamformer using two transform networks in cascade. The mathematics of basic overlapped subarray techniques is well established, but some of the analysis needs to be repeated here in order to explain the means of sidelobe reduction. Fig. 3 shows two implementations of the basic beamformer. In the sketch at left, the larger beamformer with N output terminals is a time-delay constrained lens of focal length F (possibly a Rotman or Archer lens) fed by an array of M elements (with $N \gg M$). At right, a time-delay Blass matrix is shown. Either network produces sets of progressive time-delayed signals at its output that radiate as multiple beams with beam peak locations independent of frequency. The smaller $M \times M$ multiple-beam network in the sketch at left could be an orthogonal beam network or a true time-delay constrained lens. This $M \times M$ beamformer could be replaced by a digital beamformer that replaces either of the two types of feeds. This option is emphasized in the sketch at left, where the small beamformer is omitted completely to emphasize the added compactness offered by replacing the $M \times M$ beamformer by a digital processor. It is increasingly likely that this digital option will be chosen for high-performance systems. However it is done, it will be shown later that there is a significant advantage to using a true time delayed beamformer for the $M \times M$ network.

The following analysis details are given for the equal path length (true time delay) main lens with circular back face, but all except the geometric aspects of the analysis are valid for a true time-delay multiple-beam matrix (Blass matrix). All equations except (2), (3)—(4) are equally applicable to both types of beamformers.

The lens analysis is simplified and assumes the main lens is in the far field of the feed. It also assumes a constant spacing d_L at the main aperture face and this has implications about the element patterns of the elements at the back face of that lens. These and other simplifying assumptions have been studied before [6], [7] and are shown to not alter the basic principles of operation for these networks.

For generality, assume the $M \times M$ multiple beam network can be either an orthogonal beam network (using $K = 1$) or a true time-delay lens (by using $K = \lambda_0/\lambda$). Each subarray input port "m" is fed by a signal J_m, which produces a series of signals I_{im} given by

$$I_{im} = \frac{1}{(M)^{1/2}} J_m e^{-j2\pi i(m/M)K}. \tag{1}$$

Also assume that each of these signals I_{im} can be multiplied by some weighting w_i. These signals radiate from the lens feed toward the main aperture to produce the distribution

$$A_{mn} = \frac{1}{\sqrt{N}} \sum_{i=-(M-1)/2}^{(M-1)/2} w_i I_{im} e^{+j2\pi i(dy/\lambda)\sin\phi_n}. \tag{2}$$

The angle ϕ_n, measured as shown in Fig. 3(a), relates to the focal length F and the element index "n" $-(N-1)/2 \le n \le (N-1)/2$ as

$$\sin\phi_n = n\, d_L/F. \tag{3}$$

The expression for A_{mn} has peak values equally spaced across the lens back face with the separation distance D, which corresponds to a separation defined by the beamwidth of the feed array. This spacing is frequency-dependent for the orthogonal matrix fed antenna, but constant for the time-delay feed. The distance D between any two successive maxima in the aperture illumination is given by (2) as

$$D = \frac{F}{M}\left(\frac{\lambda}{d_y}\right) K = D_0\left(\frac{\lambda}{\lambda_0}\right) K \tag{4}$$

where

$$D_0 = \left(\frac{\lambda_0}{d_y}\frac{F}{M}\right).$$

The parameter D_0 is the subarray spacing at center frequency. Since M such spacings span the lens face, then $D_0 M = d_L N$. With these substitutions, and again omitting normalizing constants, the expression for A_{mn} becomes

$$A_{mn} = \frac{J_m}{\sqrt{NM}} \sum_{i=-(M-1)/2}^{(M-1)/2} w_i \exp\left[j2\pi i\left(\frac{n}{N}\frac{\lambda_0}{\lambda} - \frac{m}{M}K\right)\right]. \tag{5}$$

In the most basic configuration, the w_i are all unity. This summation can then be done in closed form. Each subarray input port "m," fed by a signal J_m, thus produces a series of signals A_{mn} at the output of the $M \times N$ beamformer

$$A_{mn} = J_m\sqrt{\frac{M}{N}}\frac{\sin M\pi\left[\left(\frac{n}{N}\frac{\lambda_0}{\lambda} - \frac{m}{M}K\right)\right]}{M\sin\pi\left[\frac{n}{N}\frac{\lambda_0}{\lambda} - \frac{m}{M}K\right]}. \tag{6}$$

This expression shows the overlapped sinc-like aperture distribution that radiates to form a flat subarray pattern for any given Mth subarray and shows that for the orthogonal feed system ($K = 1$) the peaks of the distribution move as a function of frequency. For the time-delayed feed, however, the distribution is not orthogonal, and the location of the peaks of these distributions is independent of frequency. Four of these amplitude

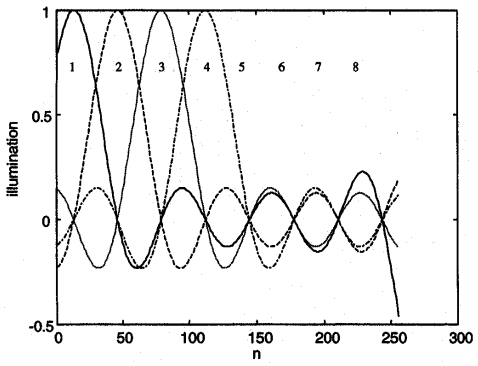

Fig. 4. Selected subarray illuminations in a section of 8 subarrays and 256 elements.

distributions are plotted in Fig. 4, for $w_i = 1$, and for a particular case of $M = 8$, $N = 256$. For reference, these distributions correspond to numbered subarrays 1, 2, 3, and 4 of the 8 subarrays within each section. To scan the subarray pattern to some angle given by $u_0 = \sin\theta_0$ requires phase shifters at the aperture. These multiply the aperture coefficients A_{mn} by $\exp(-j2\pi n u_0 d_L/\lambda_0)$. The (normalized) far-field array factor radiated from this distribution at the angle θ (with arbitrary w_i and J_m set to unity) is given below, with $u = \sin\theta$, as

$$f_m(u) = \sum_{i=-(M-1)/2}^{(M-1)/2} w_i e^{-j2\pi(m/M)Ki} \times \frac{\sin\left[(N\pi d_L)\left(\frac{u}{\lambda} - \frac{u_0}{\lambda_0} - \frac{i\,\lambda_0}{N d_L \lambda}\right)\right]}{N\sin\left[(\pi d_L)\left(\frac{u}{\lambda} - \frac{u_0}{\lambda_0} - \frac{i\,\lambda_0}{N d_L \lambda}\right)\right]}. \quad (7)$$

Element patterns have not been included in this expression.

These subarrays are all pulse-like, but not all are equally good patterns. Fig. 5 shows the four subarray patterns corresponding to the distributions of Fig. 4, with $w_i = 1$. The subarrays of this group nearer the center of the section have lower sidelobes, smaller ripples within the passband, and overall better quality for use in arraying. The subarrays near the edge of the section are more distorted, since they are more severely truncated. In accordance with the sketch of Fig. 2, the outer subarrays are simply not excited, since they are of poorer quality. So, in a system with $M = 8$, each section has only subarrays 3, 4, 5, and 6 retained, while the other ports are either not fabricated, or are terminated. For $M = 4$, only subarrays 2 and 3 are used. The selection of the "best" subarrays leads to patterns with lower sidelobes and smaller ripples in the passband, and this aids in suppressing the grating lobes located at $p\lambda/D_0$ from the main beam. Other grating lobes remain unsuppressed, and these are discussed in the next section.

B. Array Pattern of the Array with Partially Overlapped Sections

The new network partially overlaps the outputs of these sections as shown in Fig. 2, by simply adding the output signals. The array is not "fully overlapped" because each subarray distribution only extends over the length of one section. The resulting network has P subarray ports, where P is any multiple of $M/2$. The array pattern is the scalar product of the vector of complex subarray excitations with elements $J_m = |J_m|\exp(-j\pi u_0 m(D_0/\lambda - D_0/\lambda_0))$, and the vector of subarray patterns. Note that this includes phase correction to remove the phase shift that is in series with the time delay

$$F(u) = \sum_{(P-1)/2}^{-(P-1)/2} J_m f_m(u). \quad (8)$$

At center frequency, this arraying process sums subarrays that are separated by the distance D_0, and so the array factor would have grating lobes at the points $u_q = u_0 + q(\lambda_0/D_0)$, and thus are spaced 0.0625 apart in u space. These are suppressed by the subarray patterns. However, the array pattern of Fig. 1(b) (with $M = 8$) shows the expected 40-dB sidelobes near the main beam, but has a series of other quantization lobes spaced about 0.015 apart, and reaching levels of nearly -20 dB very near the main beam. Given this spacing, these near sidelobes are not due to the grating lobes of the basic subarray distance D_0, but are due to some periodicity in the array that has a period $4D_0$. They arise because the subarrays themselves occur in groups of $M/2$ (four in this case), forming a super-subarray that is undesired.

Figs. 4 and 6 help to explain this phenomenon. Within the group of four subarrays that are retained within each section, the outer two are different from the center two because of proximity to the edge of the section. The sinc-like distributions of subarrays 3 and 4 (Fig. 4) are truncated at different sidelobes, and these result in a periodicity across the array that is four subarrays wide. Fig. 6 shows a comparison of two subarray patterns (3 and 4 of an eignt-element group), to emphasize their slight amplitude differences. The subarray pattern phases (not shown) also have different ripples about the phase center. These amplitude and phase differences mean that the set of subarrays 3, 4, 5, and 6 form the grouping that is repeated by adjacent sections, and so determines a periodicity of $4D_0$. The resulting sidelobes (grating lobes or quantization lobes) are not large, and as the array is scanned they vary from the -15 to -20-dB level. They occur within the subarray passband, where they are caused by the differing ripples shown at the top of the passband, and within the subarray sidelobe region. They can be reduced further by making all the subarray patterns nearly identical (so that each group is nearly identical to every other). Then, at center frequency, the only periodicity is the subarray spacing D_0, and any quantization lobes should be outside of the subarray passband.

C. Sidelobe Control Using the Method of Alternating Projection

The subarrays can be made more similar by inserting a special set of in-phase weights between the two transform networks.

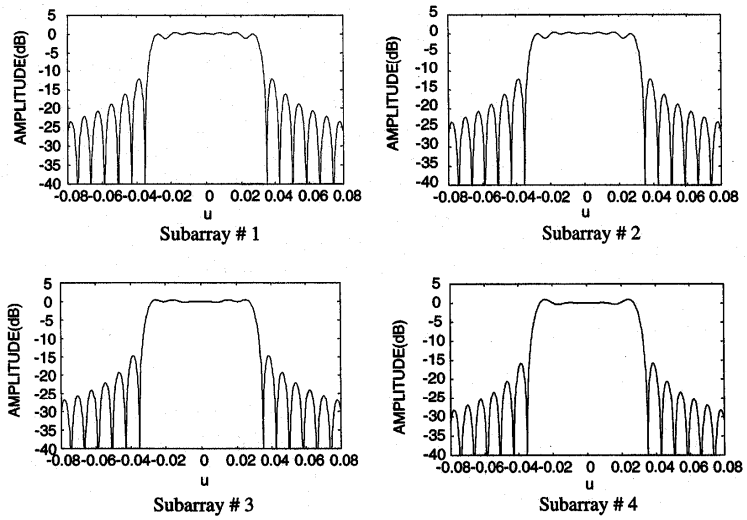

Fig. 5. Selected subarray radiation patterns for a section of 8 subarrays.

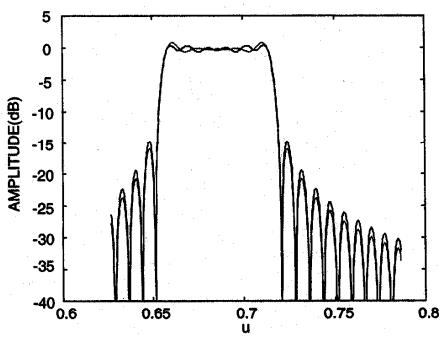

Fig. 6. Radiation patterns of subarrays 3 and 4 of section with eight subarrays.

The logic for employing this procedure is as follows. With uniform illumination at the feed, the feed array radiates to the main lens face in a sinc-like distribution with sidelobes at the -13-dB level. Altering the weights w_i with, for example, a tapered distribution would produce a lower sidelobe illumination at the main lens and so perhaps a distribution that would not be so seriously impaired by truncation. Minumizing truncation thus makes the subarray patterns more similar and essentially eliminates the periodicity of length $4D_0$. A procedure is introduced below to select the proper weights w_i that produce a low sidelobe distribution.

The method of alternating projections [8], [9] (also called the intersection approach) as it is applied to antenna pattern synthesis, depends on the finite Fourier transform relationship between an array illumination and its far-field pattern. The "projection" of a point (function) in one vector space onto another vector space is a point in the second space with minimum error subject to some chosen norm. For an N-element array, the Fourier series synthesized array pattern is the projection of this set of all possible N-element array patterns onto the set of (in this case) one desired pattern, since its mean square error is minimum. The procedure, as outlined schematically in Fig. 7 for subarray synthesis, consists of iterating a sequence of "projections" between two vector spaces (sets of functions). In this case, one set (set A) is the set of all subarray patterns that can be radiated by the weights w_i acting as feed for the lens. The second set of functions (set B) is the set defined by all the patterns that lie between the masks [8], which are the upper and lower bounds for the subarray pattern, and shown on that figure as between M_U and M_L In this case, the projection of set A onto B is obtained by producing a new pattern f_0' such that every point of the original f_0, whose magnitude lies outside of the mask, is moved to the nearest mask limit M_U or M_L. This is the nearest pattern to set B, and the projection of the pattern in set A onto set B. So, values of the subarray pattern amplitude $>M_U$ are made equal to M_U, values $<M_L$ are made equal to M_L, and points within the bounds are unchanged. Fig. 7 illustrates this operation, with the resulting projection being the solid curve in the upper right of the figure.

For convenience, we assume temporarily that the $M \times M$ matrix has one beam that radiates broadside (call it $m = 0$, and assume $u_0 = 0$, and center frequency $\lambda = \lambda_0$). This beam has signals $I_i = 1$ (normalized) for all i. Assume that weights w_i now multiply the signals I_i. These radiate to the lens back-face, and (7) gives the radiated subarray pattern. For convenience, 800 far field points are used to define the subarray pattern. This

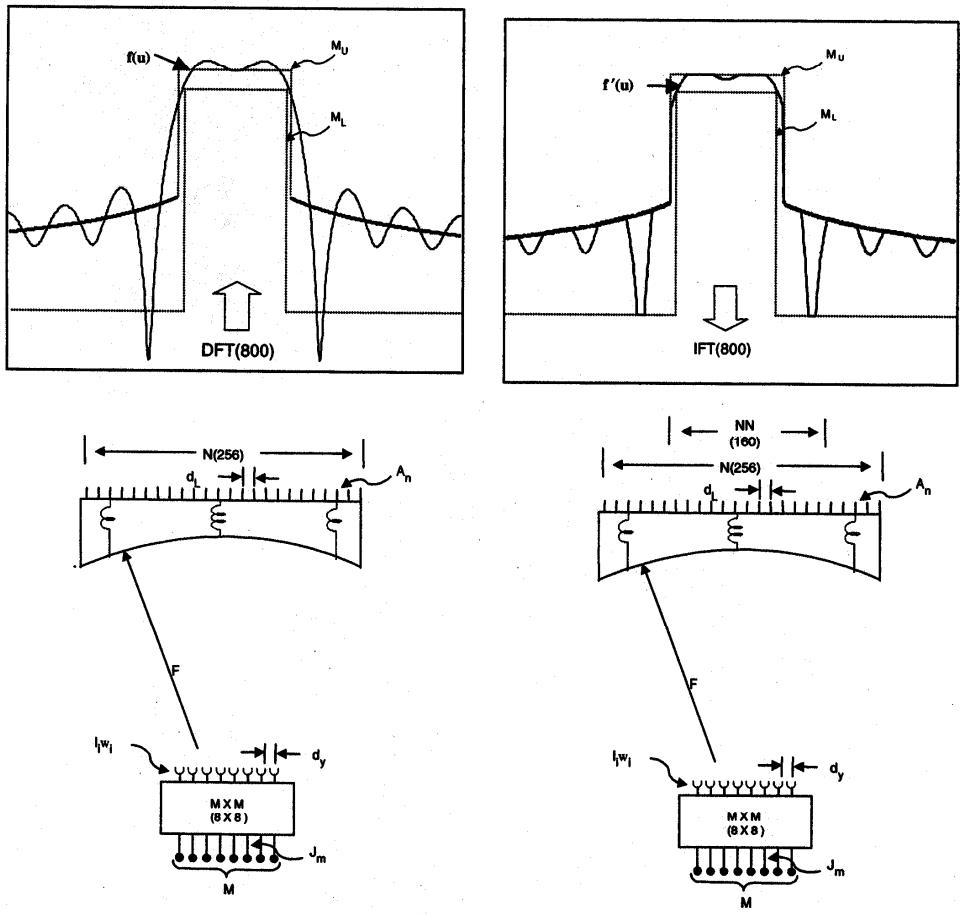

Fig. 7. Alternating projection method used to reduce subarray truncation by iterating weights w_i.

pattern belongs to one vector space, called space A above, and an example shown in the upper left of Fig. 7.

Next, this radiated subarray pattern (top left) is projected onto the desired mask, having an upper limit M_U of width $\lambda_0/D_0 = 0.0625$ and a lower limit M_L of width about one third of the upper limit width. This projection is sketched in the top right of the figure. The inverse finite Fourier transform (Fourier series) of this far field $f'(u)$ yields a set of illuminations A'_{0n} on the ens (lower right figure) given by the expression below.

$$A'_{0n} = \frac{d_L}{\lambda} \int_{-\lambda/2d_L}^{\lambda/2d_L} e^{-j2\pi nu(d_L/\lambda)} f'(u) du. \qquad (9)$$

In practice, this expression is evaluated using 800 points of the discretized $f'(u)$.

The essence of the synthesis procedure is to impose the constraint that the illuminated lens aperture be smaller than the original ($N = 256$) elements. Choosing a smaller lens avoids illuminating the edges of the larger lens with the sidelobes of the aperture distribution of the outermost subarrays. In a section of 256 elements with 8 subarrays, discarding the outer two on each side leaves subarrays 3 and 6 as the outermost ones, and their centers are $2.5D_0$ (or 80 elements) from each side for 32-element subarrays. So, one could formulate a new subarray synthesis situation to produce an illumination for a single subarray that radiates with a flat top and is confined to a smaller lens, one 160 elements wide. Confining the central subarray to this smaller aperture becomes a constraint on the synthesis problem and assures that the aperture illumination for subarrays 3 and 6 terminate at the edge of the original 256 element lens. For

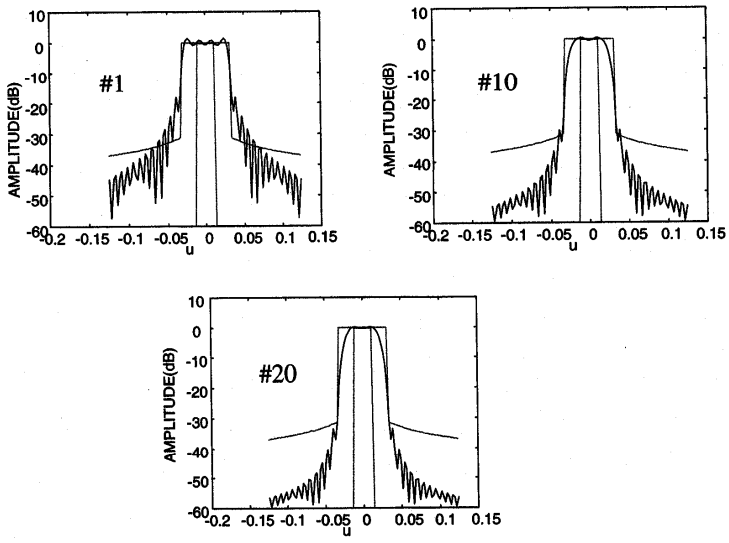

Fig. 8. Iterative sequence showing convergence within mask boundaries.

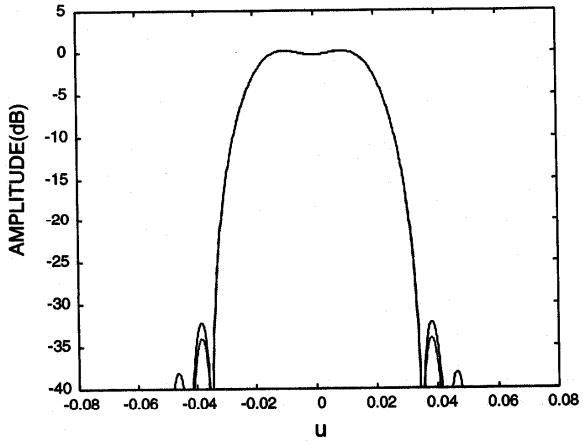

Fig. 9. Radiation patterns of subarrays 3 and 4 of section with 8 "optimized" subarrays.

a section with $M = 4$, the central two subarrays are $1.5D_0$ (48 elements) from the edge. In that case, a trial lens would be $48 \times 2 = 96$ elements wide. The procedure chosen to affect this synthesis is a variation of the technique called alternating vector space projections. In keeping with the previous discussion, we use $NN = 160$ instead of the 256 elements in the real lens. This is one constraint put on the solution of the synthesis procedure.

These A'_{0n} may not be achievable, given the only eight possible values of the w_i coefficients, but they can be approximated optimally since they are related to the w_n through the inverse transform. These A'_{0n} are projected back through the network to the front of the $M \times M$ network using the factor

$$w_i = \frac{1}{\sqrt{N}} \sum_{-(NN-1)/2}^{(NN-1)/2} A_{0n}{}' e^{-j2\pi in/N}. \qquad (10)$$

Equation (10) is the inverse of the transform (2), using (3) and (4). Having w_i, (7) can again be used to compute the subarray

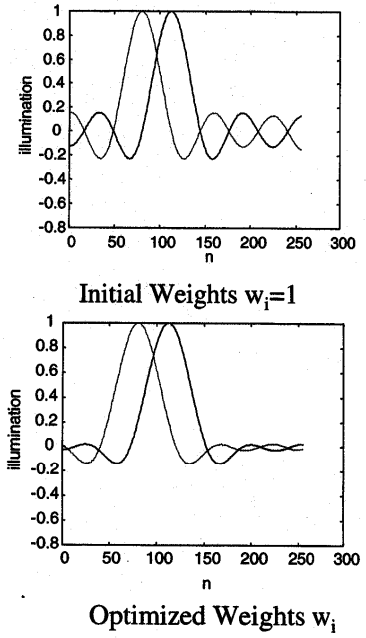

Fig. 10. Comparison of real aperture illuminations using initial weights w_i and "optimized" weights w_i.

pattern. This completes one cycle of the iteration. Fig. 8 shows the computed subarray patterns for four specific iterations, starting at iteration #0, the initial pattern with all weights unity, and ending at iteration #20. In this sequence, the outer mask is the upper mask function shown, and chosen to be the width 0.0625 in u-space, and to have near sidelobes at approximately the -30 dB is level, and decaying following a $1/(|u - u_0|)$ asymptote. Convergence is evident from the examples shown in the figure.

In this case, at the end of the synthesis procedure, the final weights were $w_1 = w_8 = 0.291$; $w_2 = w_7 = 0.753$; $w_3 = w_6 = 1.006$; $w_4 = w_5 = 0.982$. Most likely, these weights are implemented digitally since they can readily be incorporated in a digital beamformer which also does the smaller $M \times M$ Fourier transform.

Fig. 9 shows the power patterns of subarrays 3 and 4 (or 6 and 5), computed directly from the final weights given above. Clearly the procedure has made the subarrays nearly identical down to the -32-dB level. The subarrays also have lower sidelobes, because of the reduced truncation.

Fig. 10 compares the aperture illuminations using the initial (uniform) weights ($w_i = 1$) and the synthesized weights for two adjacent subarrays of the central four. The primary constraint imposed by the synthesizing procedure was to assure that this illumination was little effected by truncation. Indeed, the lower figure has far smaller ripples and so the radiation patterns of the subarray at left (dotted) are very similar to the one at right (solid).

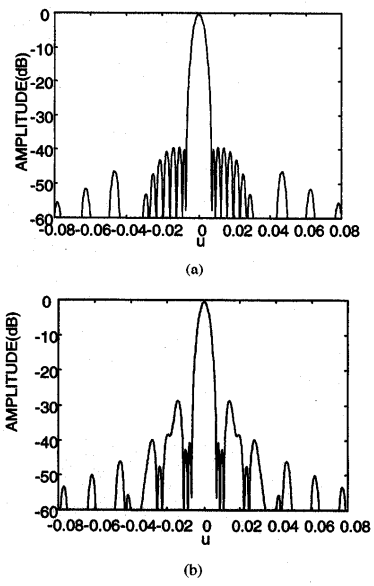

Fig. 11. Broadside radiation patterns of array of 4 "optimized" partially overlapped sections with 16 subarrays, and using orthogonal feed matrices ($M = 8$). (a) $f/f_0 = 1$. (b) $f/f_0 = 1.03$.

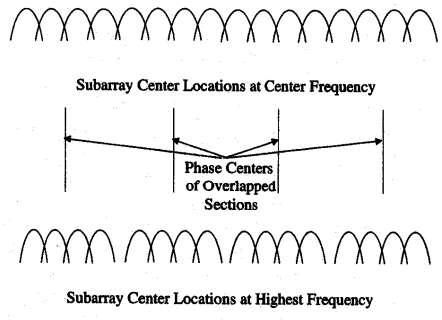

Fig. 12. An example of subarray clustering for orthogonal (phase shift) feed matrix.

Fig. 11(a) shows the center frequency broadside patterns of an array of four sections, each with eight subarrays, but using the central four and choosing the synthesized weights. This pattern shows the advantage of the subarray synthesis procedure, demonstrating sidelobes at the -40-dB design level, and all residual grating lobes below -45 dB. Notice that these remaining lobes are still spaced about 0.015 apart, indicating that they arise from the periodicity $4D_0$.

Although no distinction has been made thus far concerning the use of an orthogonal beamformer (Butler Matrix) or a true time-delay beamformer (Rotman Lens) or their analog or digital equivalents, for the $M \times M$ beamformer, there is in fact a major difference in the frequency response. Fig. 11(b) shows that the

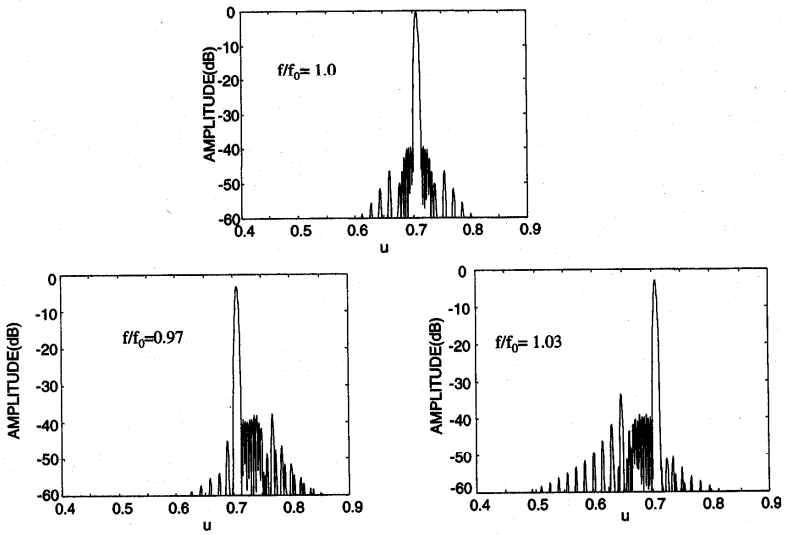

Fig. 13. Radiation patterns of array of Fig. 11 at center frequency and band edges (6% bandwidth).

broadside radiation pattern of the network fed by an orthogonal beamformer at frequency $f = 1.03f_0$ has significant sidelobes at $u = \pm 0.0625 f_0/(4f) = \pm 0.0152$ not present at center frequency. Fig. 12 illustrates schematically that this problem results from the choice of an orthogonal beamformer as feed, not a true time-delay beamformer. With the orthogonal beamformer at center frequency, the subarray amplitude and phase centers are evenly spaced in all of the four sections, and the sections are exactly four subarrays apart to produce an aperture distribution with periodicity equal to the subarray separation. However, with the orthogonal beamformer, the angle between beam peaks varies inversely with frequency. The cluster of beams that excite each section has its phase center at the physical center of the section and the whole cluster gets narrower as the frequency increases. Fig. 12 shows the radiation peaks moving toward the broadside direction at the highest frequency. Since each group of four has its phase center at the center of a section, the sketch at bottom shows there is imposed a periodicity of $4D_0$ across the array at frequencies above the design center frequency.

This periodic error is removed when a true time delay or digital beamformer is used as beamformer. The beams from these time-delayed networks remain equally spaced on the final aperture, and the $4D_0$ periodicity is removed. Fig. 13 shows the resulting array patterns at center frequency and at 0.97 and 1.03 times the center frequency. In all cases, the large quantization lobes are removed, and the sidelobes are in the neighborhood of -35 dB, increasing to -32 dB at the high end of the band. This 6% bandwidth represents 70% of the theoretical maximum bandwidth for the given subarray spacing. These results confirm that it is possible to reduce all sidelobes to very low design levels using this synthesis technique.

Additional data, not shown, at 0.965 and 1.035 times the center frequency, have sidelobes at approximately 26 dB below the main beam. These limits represent 82% of the theoretical maximum bandwidth.

D. Results for a 24% Bandwidth Array

Fig. 14 shows the results of simply scaling all dimensions to produce an array of the same size with 4 times the bandwidth of the 6% system. Accordingly, setting $D_0 = 4\lambda_0$ instead of 16, and broadening both mask boundaries by the factor 4, reducing the section size N by four, and increasing the number of sections by four, one gets an array of 64 subarrays (requiring 64 instead of the previous 16 time delay units). The figure shows grating lobe reduction comparable to the 6% case, and good operation over the larger bandwidth.

It is important to note that increasing the bandwidth has reduced the size of each section by the factor four. If the network is built with lenses, the depth of the structure is also reduced by four. The resulting section size for this 24% configuration is $N = 64$, a size that can be achieved quite compactly with stripline Rotman (Archer) lenses.

E. Results for a 6% Bandwidth Array Using Sections of Four Subarrays ($M = 4$)

Fig. 15 shows the final radiation patterns for an array made up of 32 subarrays, of 32 elements each, but using eight sections of four, instead of four sections of eight. The advantage of this configuration is compactness. If the sections have lens front faces, then the lens dimension and the number of elements in the lens face are reduced by two and make the technology simpler. For

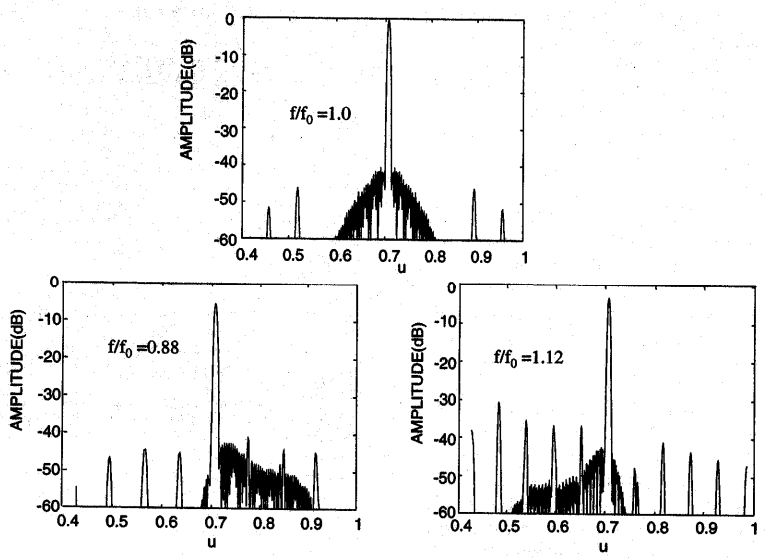

Fig. 14. Radiation patterns at center frequency and band edges of array of 16 partially overlapped sections with 64 subarrays (24% bandwidth).

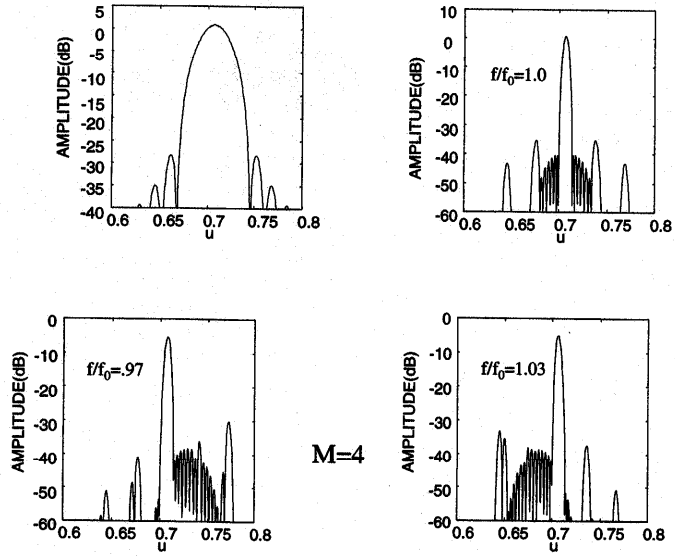

Fig. 15. Radiation patterns at center frequency and band edges for array of eight sections of four subarrays each. (6% bandwidth). Subarray pattern at center frequency shown upper left.

example, in this 6% bandwidth case, the lens face has 128 elements instead of 256, and is only one half as deep. This makes lens development much easier.

This configuration also has a significant advantage if the output beamformer were a true time-delay Blass matrix, for then each section would reduce to a two beam Blass matrix, since the beams 1 and 4 would not be excited.

The penalty for using this compact geometry is that, with four subarrays and (because of symmetry) only two degrees of freedom, one cannot tailor the subarray pattern to maintain a

flattened top while synthesizing subarrays 2 and 3 to be nearly equal. The resulting subarray patterns (both overlayed at the top left of Fig. 15) are identical in amplitude and nearly so in phase, but have rounded tops and less steep skirts than the $M = 8$ design. This results in sidelobe levels of approximately -26 to -27 dB over the 6% bandwidth, but raises to approximately -18 dB at the edges of the 7% bandwidth.

III. Conclusion

Using an alternating projection technique to synthesize network weights, a new subarraying technique that uses constrained network feeds has been shown to enable the insertion of true time-delayed signals without resulting in high sidelobes or grating lobes. The technique is expected to find application to arrays with volume restrictions, such as space-based or airborne radar.

This paper has demonstrated sidelobe reduction to the -40-dB level and a bandwidth of approximately 70% of the maximum theoretical bandwidth.

In terms of its practical implementation, the technique imposes a 3-dB combining loss beyond what one would have with a conventional power divider network and contiguous subarrays. The technique is therefore useful as a feed for an array of columns, where one would naturally have amplification or TR modules. In most arrays of this type, the loss would bring little disadvantage. The depth of the network shrinks as the bandwidth is increased, since then more time delays are used for scanning. Various alternate networks, such as constrained Blass matrices or smaller ($M = 4$) sections, further reduce the array volume.

In summary, the technique allows large subarrays to be used to insert time-delay scanning of array patterns while maintaining low sidelobes. The subarrays are up to 32 elements wide for 6% bandwidth and 8 elements wide for 24% bandwidth. This represents a substantial reduction in the number of time delay units, amplifiers, and other devices in comparison with conventional approaches, and it offers the lowest sidelobes of any constrained feed subarraying network yet reported.

References

[1] R. Tang, "Survey of time-delay steering techniques," in *Phased Array Antennas*. Dedham, MA: Artech House, 1972, pp. 254–260.

[2] S. P. Skobelev, "Methods of constructing optimum phased array antennas for limited field of view," *IEEE Antennas Propagat. Mag.*, vol. 40, pp. 39–50, Apr. 1998.

[3] R. J. Mailloux, "Periodic arrays," in *Antenna Handbook*. New York: Van Nostrand Reinhold, 1988, ch. 13, pp. 13-1–13-68.

[4] ——, "Constrained feed technique for subarrays of large phased arrays," *Electron. Lett.*, vol. 34, no. 23, pp. 2191–2193, Nov. 1998.

[5] ——, "Constrained feed techniques for limited field of view scanning or time delay steering," in *Proc. IEEE AP-S Int. Symp.*, 1998, pp. 740–743.

[6] R. L. Fante, "Systems study of overlapped subarrayed scanning antennas," *IEEE Trans. Antennas Propagat.*, vol. AP-28, pp. 668–679, Sept. 1980.

[7] H. L. Southall and D. T. McGrath, "An experimental completely overlapped subarray antenna," *IEEE Trans. Antennas Propagat.*, vol. AP-34, pp. 465–474, Apr. 1986.

[8] O. Bucci, G. Franceschetti, G. Mazzarella, and G. P. Panariello, "Intersection approach to array pattern synthesis," *Proc. IEEE*, pt. H, vol. 137, pp. 349–357, Dec. 1990.

[9] O. Bucci, G. Mazzarella, and G. Panariello, "Reconfigurable arrays by phase-only control," *IEEE Trans. Antennas Propagat.*, vol. 39, pp. 919–925, July 1991.

Robert J. Mailloux (S'57–M'66–SM'72–F'78) received the B.S. degree in electrical engineering from Northeastern University, Boston, MA, in 1961 and the S.M. and Ph.D. degrees from Harvard University, Cambridge, MA, in 1962 and 1965, respectively.

Currently, he is a Senior Scientist at the Sensors Directorate, Air Force Research Laboratory, Hanscom Air Force Base, MA. He has served as the Chief of the Antennas and Components Division, Rome Laboratory, and as a Physicist with the Air Force Cambridge Research Laboratory. He is the author or coauthor of numerous journal articles, book chapters, and *Phased Array Handbook* (Norwood, MA: Artech House, 1994). His research interests are in the area of periodic structures and antenna arrays.

Dr. Mailloux was President of the Antennas and Propagation Society in 1983. In 1992, he received the IEEE Harry Diamond Memorial Award and recently received the IEEE Third Millennium Medal. He is a member of Tau Beta Pi, Eta Kappa Nu, Sigma Xi, and Commission B of the International Scientific Radio Union. He has been a distinguished Lecturer for the Antenna and Propagation Society and is currently Chairman of the AP-S/IEEE Press Liaison Committee.